January 2019

Evaluation Of Rutting And Cracking Resistance Of Fiber Reinforced HMA Mixes In North Dakota

Zeenat Nahar

EVALUATION OF RUTTING AND CRACKING RESISTANCE OF FIBER REINFORCED HMA MIXES IN NORTH DAKOTA

by

Zeenat Nahar

Bachelor of Science, Shahjalal University of Science & Technology, 2013

A Thesis

Submitted to the Graduate Faculty

of the

University of North Dakota

In partial fulfillment of the requirements

for the degree of

Master of Science

Grand Forks, North Dakota

August

2019

This thesis, submitted by Zeenat Nahar in partial fulfillment of the requirements for the Degree of Master of Science from the University of North Dakota, has been read by the Faculty Advisory Committee under whom the work has been done and is hereby approved.

Dr. Nabil Suleiman,

7/29/2019

Dr. Daba Gedafa

Sukhvarsh Jerath 7/25/2019

Dr. Sukhvarsh Jerath

This thesis is being submitted by the appointed advisory committee as having met all of the requirements of the School of Graduate Studies at the University of North Dakota and is hereby approved.

Grant McGimpsey,
Dean of the Graduate School

7/30/19

Date

PERMISSION

Title	Evaluation of Rutting and Cracking Resistance of Fiber Reinforced HMA Mixes in North Dakota
Department	Civil Engineering
Degree	Master of Science

In presenting this thesis in partial fulfillment of the requirements for a graduate degree from the University of North Dakota, I agree that the library of this University shall make it freely available for inspection. I further agree that permission for extensive copying for scholarly purposes may be granted by the professor who supervised my thesis work or, in his absence, by the chairperson of the department or the dean of the Graduate School. It is understood that any copying or publication or other use of this thesis or part thereof for financial gain shall not be allowed without my written permission. It is also understood that due recognition shall be given to me and to the University of North Dakota in any scholarly use which may be made of any material in my thesis.

Zeenat Nahar
July 10th 2019

TABLE OF CONTENTS

Page

Page

LIST OF TABLES

LIST OF FIGURES

ACKNOWLEDGMENTS

I would like to express my regards to my advisor, Dr. Nabil Suleiman for all the supports, encouragements, and counseling he provided during my master program.

I would also like to extend my gratitude to the members of my graduate committee: Dr. Daba Gedafa and Dr. Sukhvarsh Jerath for their help.

To my husband Akkas Uddin Haque, who has been a very supportive partner and to my parents – my inspiration behind all my good works

ABSTRACT

Asphalt pavements deteriorate over time due to traffic loads and weather conditions. The primary failure modes of asphalt pavements in North Dakota are rutting, fatigue cracking, and low temperature cracking. This study investigated whether the addition of Aramid Fiber to SuperPave HMA mixes improves their resistance to rutting, low temperature cracking, and fatigue cracking. The experiments were conducted on conventional and fiber mixes provided by the North Dakota Department of Transportation. The Asphalt Pavement Analyzer (APA), Disk Shaped Compact Tension (DCT), and the Semi-Circular Disk Shape equipment (SCB) were used to test for rutting, low temperature cracking, and fatigue cracking resistances, respectively. Study findings indicate that the addition of Aramid fiber to SuperPave HMA mixes did not improve the rutting resistance of the HMA mix. Significant increase in fatigue cracking resistance was observed in the fiber mix while a decrease in low temperature cracking resistance was seen due to the addition of fiber.

CHAPTER 1

INTRODUCTION

1.1 Background

Approximately 94 percent of roads and highways in the United States are asphalt pavements. The state of these pavements deteriorates due to traffic load and weather condition which results into rutting, low temperature cracking and Fatigue cracking(Muftah et al., 2017).

To mitigate the rutting and cracking in the asphalt pavement, the addition of fiber in HMA has been done in the past to provide additional tensile strength and fracture energy to the asphalt pavement. Aramid is a unique fiber which has tensile strength of 400,000 psi. It has micro-roots which help to anchor themselves into the finished HMA. During summertime when asphalt gets hot and tends to rut under load, the rooted Aramid Fibers provide resistance to the "flow" of the in-place asphalt which helps to minimize rutting. During wintertime, when asphalt tends to shrink because of cold, Aramid Fibers provide added tensile strength for resistance to cracking(Tech, 2019; Muftah et al., 2017).

Tests were done on Aramid Fiber – reinforced mix and on Conventional HMA. Both the conventional and fiber-reinforced HMA loose mixes for conducting experiments were provided by North Dakota department of Transportation (NDOT).

The provided loose mixes were first reheated in the oven at the temperature of 290F.The loose mixes were then compacted in the lab to prepare samples for testing. $7 \pm 1\%$ air voids have been considered while preparing samples. The Asphalt Pavement Analyzer (APA), Disk Shaped Compact Tension (DCT), and Semi-Circular Bending(SCB) equipment were used to test the specimens for rutting, low temperature cracking, and fatigue cracking, respectively.

1.2 Hypothesis

It is hypothesized that the addition of Aramid fiber in asphalt mixture provides resistance to rutting and provide tensile strength for resistance to cracking.

1.3 Scope of the Study

The traditional and fiber-reinforced mixes were used for the research. The only difference for these mixes was the addition of Aramid fibers for the fiber-reinforced samples.

The Specimens that were used for testing are listed as follows:

1. Four sets of specimens have been tested for the APA experiment. The specimens that have been used for the conventional samples are – no. 10, no. 11, no. 19, no. 20 and for fiber-reinforced samples are – no. 3F, no. 5F, no. 6F, no. 7F. AASHTO T340-10 protocol has been followed for the APA testing.

2. Four sets of specimens have been tested for the DCT experiment. The specimens that have been used for the conventional samples are – no.2, no.6, no. 15, no.17

and for fiber-reinforced samples are – no. 20F, no. 21F, no. 22F, no. 24F. ASTM D7313-13 protocol has been followed for the DCT testing.

3. Four sets of specimens have been tested for the SCB experiment. The specimens that have been used for the conventional samples are –both parts of no.1 and no.6, no. 2 no.17 and for fiber-reinforced samples are – no. 8F, no. 10F, no. 12F, no. 16F. ASTM D7313-13 protocol has been followed for the SCB testing as well.

P.S. - The letter "F" next to a number indicates that it's a fiber-reinforced sample

1.4 Organization of the Thesis

The objective of this study was to compare and determine whether the addition of Aramid fiber to SuperPave HMA mixes creates significant impacts in rutting, low temperature cracking and fatigue cracking resistance than traditional HMA mixes.

1.5 Study Outline

The thesis is separated into five chapters

1. **Chapter 1: Introduction** The introduction includes background information on Aramid fiber in asphalt pavement, hypothesis, scope of the study and study objectives.

2. **Chapter 2: Literature Review** This chapter is divided into three sections – rutting in asphalt, low temperature cracking in asphalt, fatigue cracking in asphalt.

3. **Chapter 3: Methodology** This chapter discusses material selection, mix design, compaction methods ans testing. Under mix design, the chapter discusses the composition and specification of the mixes as provided by the North Dakota Department of Transportation(NDDOT). It also discusses the volumetric properties of the samples used for the testing. Three different testing methods are discussed: Asphalt Pavement Analyzer (APA), Disc Shaped Compact Test and Semi Circular Bend Test.

4. **Chapter 4: Results and Discussion** This chapter tabulates the results obtained from the work and provides inference based on the results

5. **Chapter 5: Conclusions and Recommendations** The chapter summarizes the results and discusses the limitations of the work. It also provides an idea on the how the work could be extended in future experiments.

CHAPTER 2

LITERATURE REVIEW

2.1 Rutting in Asphalt

Rutting of asphalt pavement is the process of permanent deformation that occurs in the pavements typically through repeated movement of vehicles on the pavement over an extended period of time. The cause of rutting is mainly the fact that the aggregate and binder material in asphalt roads are able to move. Vehicles moving on the pavement are not the only cause of rutting. Poor asphalt mixes, inadequate thickness of pavements, and insufficient compaction can all lead to rutting. Pavement thickness becomes the primary concern when the subbase is not adequately thick or is soft, thus making the material is more prone to be easily depressed. Rutting can be reduced significantly if a stronger and stiffer subbase is used(Liley, 2018).

Rutting occurs over time, as cars are continuously driven over asphalt, the tires continue to depress the asphalt, which is then pushed outwards along the tire sides. Poor asphalt mixes are also a major cause of rutting. Excess asphalt in the mixture makes the mix more malleable which makes it more prone to rutting. Measurements need to be kept precise and sharp to avoid adding excess asphalt(Liley, 2018).

Rutting can lead to hazardous conditions on pavements. Hydroplaning can be caused from water being held in the depressions which could lead to an increase in the likelihood of vehicle accidents. Replacing roads with ruts is expensive and

frequent replacements of roads contributes to economic loss. In figure 2.1 we can see that the surface of the main road between Częstochowa and Katowice in Poczesna has been depressed by 14 cm which is defined as 14 cm Rut on the road surface.

Figure 2.1. On a road between Katowice and Częstochowa in Poczesna, a large 14 cm rut is clearly visible(Wikipedia, 2019)

The three components of hot mix asphalt on which rutting depends on are aggregate, asphalt cement,and air void. To strengthen asphalt pavements against rutting damage, modifiers are added to the asphalt binder. Fiber can help to stabilize the asphalts by making the asphalts stick to the surface of the fibers and hinder the flowing of asphalts at elevated temperatures(Xu et al., 2010). It does this by forming a three dimensional mesh in the matrix of asphalt. This resists shear force and reduces fluidity by reinforcing the structure. However, excess fiber tends to clump creating points of weakness in the mixture of asphalt and concrete. This reduces the interlocking property of fibers and thus reduces rutting resistance. Cracking is better resisted

by choosing a fiber of more tensile strength. Fibers with more length to diameter ratio leads to a stronger interlocking mechanism and thus a stronger matrix(Fu et al., 2000).

2.2 Asphalt Cracking in Low Temperature

In cold weather climates, the main cause of distress in asphalt pavements is low temperature cracking. The pavement, due to its thermal properties, tries shrinking with the drop in temperature. This leads to the building up of stress upto a point ultimately leading to formation of cracks. These cracks can be formed either by a single cooling cycle or over the course of multiple alternating cooling and warming cycles. The cracks are then widened by being subjected to vehicular loads or lower temperatures(Park et al., 2015).

The cracking is asphalts are mainly divided into two main groups based on how they are formed : (1)single event cracks and (2) thermal fatigue cracks. The first one occurs due to quick cooling in very cold climates. The second one develops over the course of alternating cooling and warming cycles and tend to occur in places with milder climates where there is a greater amount of daily fluctuations in temperature(Marasteanu et al., 2007).

As shown in figure 2.2, thermal cracking is manifested in the form of equally spaced, parallel and transverse oriented pavement cracks. Thermal stress builds up with the decrease in temperature as the asphalt in the pavement contracts. The stress distribution is not uniform throughout the thickness of the pavement as shown

in figure 2.2(b). The greatest stress is at the surface of the pavement which leads the cracks to be initiated at the surface(Marasteanu et al., 2007).

Typical pattern of low temperature cracking in Asphalt pavement is shown in figure 2.2(a). Formation of Thermal cracks and depiction of the un-uniform distribution of stress along the thickness of the pavement is shown in 2.2(b).

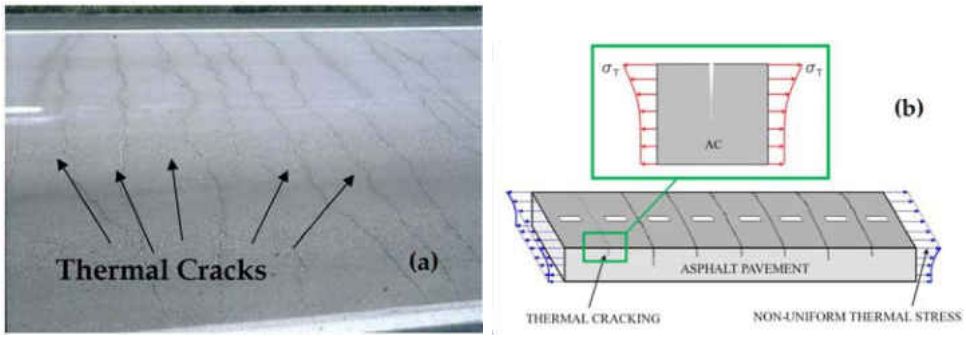

(a) (b)

Figure 2.2. Cracking due to low temperature in asphalt pavements (a)Typical pattern of low temperature cracking in Asphalt pavement (b) Formation of Thermal cracks and depiction of the un-uniform distribution of stress along the thickness of the pavement.(Marasteanu et al., 2007)

To improve resistance to cracking of asphalt concrete pavement, modifiers like fiber has been added to the asphalt content and its effects recorded using the indirect tension test at cold temperatures in past studies. Cracking resistance at cold temperatures of asphalt mixes can be improved efficiently by the addition of steel fibers in the mix. The interlocking mechanism of the fibers increases the resistance of fibers to pull out of the matrix thus increasing the tensile strength upto a critical diameter of fiber, beyond which there is little effect of fiber(Park et al., 2015).

2.3 Fatigue Cracking in Asphalt

Fatigue cracking, which is also called alligator or crocodile cracking which usually tend to look like connected cells much like the scales of a reptile. If the fatigue cracks appear in asphalt pavement, the damage to the pavement can become extensive rapidly and deteriorate vast portions of the pavement in a short period of time. Fatigue cracking happens if the supporting foundation of the pavement is not able to support the mass of traffic(AlphaPavingTexas, 2019)..

Asphalt pavement is built in such a way as to bear a given number of vehicles and classes of vehicles based on weight. The loads that the pavement is expected to be subjected to decide the foundation thickness and the asphalt depth. For instance, a busy highway bears different types of loads than a driveway. Likewise, major arterials are built to support loads that are not generally supported by residential streets. Fatigue cracking occurs when a pavement is used to support greater loading than it was built to do. This is why parking lots designed for passenger vehicles become prone to fatigue cracking when subject to the greater loading from trucks that are heavily loaded. This type of cracking is also developed in detour roads through side streets during the repair of a major arterial(AlphaPavingTexas, 2019).

Water penetration is the major cause of an eroded foundation. Eroded foundations are one of the major causes of fatigue cracking. When potholes and cracks are not quickly repaired, water penetration occurs. When water penetrates through the cracks in the pavement, water can seep through to the foundation and thus cause it to become unstable. Water penetration can also be caused by clogged drains or runoff

from nearby elevated regions which would allow the water to enter through the edges of the pavement(PavementInteractive, 2019b).

Figure 2.3 shows severely fatigued cracked asphalt pavement road where that cracking pattern looks like the back of an alligator which is why fatigue cracking is also known as Alligator cracking.

Figure 2.3. Very severely fatigued cracked pavement(PavementInteractive, 2019a)

Fiber is mainly used to increase the tensile strength of the pavement composite. They could contribute to the increasing the maximum stress that the mix could be subject to during the fracture and fatigue processes(Mahrez et al., 2003). Fiber Reinforced Bituminous Mix (FRBM) is generated through the addition of different types of fibers to the aggregates and binder while preparing the mix. FRBMs demonstrate

a great resistive properties to fatigue cracking, aging, bleeding, as shown by Brown and Maurer (1989); Serfass and Samanos (1996). Mixes reinforced with asbestos show higher resistance to fatigue stress and also don't exhibit a reduction of voids on account of traffic(Huet, 1990). Porous bituminous mixes with cellulosee fibers were observed to be exhibiting similar properties.

CHAPTER 3

METHODOLOGY

3.1 Material Selection

The fiber and non-fiber loose mixes provided by NDDOT were used to conduct experiments for low temperature cracking, rutting, and fatigue cracking. The differences between the loose mixes is only the addition of fiber in asphalt content. Gyratory Compactor, Disk Shaped Compact Tension (DCT), Semi-Circular Disk Shape (SCB) and Asphalt pavement analyzer (APA), methods were used for the test procedures.

3.2 Mix Design

The mix design for project NHU-SS-TRP-2-020(016)001 was provided by North Dakota Department of Transportation(NDDOT). Mix design properties for both Fiber Reinforced HMA mixes and No Fiber HMA mixes are provided in Tables 3.1, 3.2, and 3.3. The main properties of the Superpave are - Superpave mix design, asphalt binder performance grade and aggregate properties.The performance grade (PG) for the Superpave hot mix design is 58 -28 which means the highest physical temperature of the binder must be up to 58°C and the lowest temperature should be down to -28°C. Aggregate properties of Superpave are 2 types - consensus properties and source properties. Flat and elongated particles, fine aggregate angularity, coarse

aggregate angularity, and clay content comprise consensus properties. Properties like deleterious materials, soundness, and toughness comprise source aggregate (Zumrawi and Edrees, 2016). The aggregate properties for the mix design has been provided in Table 3.1.

Table 3.1
Mix Properties at Recommended Asphalt Content

Sl. No.	Property	Mix Design	Specification
1	Optimum AC (%)	5.5	NA
2	Density (pcf)	145.8	NA
3	Air Voids (%)	4	2.0 – 6.0
4	VMA (%)	14.1	14.0min
5	VFA (%)	71.3	65 - 78
6	%Gmm @ Ninitial	88.3	89max
7	%Gmm @ Nmaximum	97.1	98max
8	AC Film Thickness (m)	8.1	7.5 - 13
9	Dust/Effective AC Ratio	1.2	.6 - 1.3
10	Fine Aggregate Angularity (%)	43	43min
11	Sand Equivalent (%)	54.3	40min
12	Coarse Aggregate Angularity (%)	89.3	75min
13	Flat/Elongated Pieces (%)	0	10max
14	Virgin Add AC (%)	4.1	

Table 3.1 shows optimum asphalt content percentage for the fiber and conventional mix is 5.5. VMA stands for Voids in Mineral Aggregate which is the air-void spaces that exist between the aggregate particles in a compacted paving mixture, including spaces filled with asphalt(Kandhal et al., 1998). 14.1% is the VMA percentage recommended according to the table. VFA stands for the voids filled with asphalt in compacted aggregate mass.

Aggregate gradation in the HMA mix design is influential as it has potential impacts on stiffness, stability, durability, permeability, workability, fatigue resistance, frictional resistance and resistance to moisture damage (Roberts et al., 1991). Excessive fine gradations (naturally occurred or caused due to excessive abrasion) cause distortion. Because if the fine particles are in large amounts, then they are inclined to push the larger particles apart and as a result they perform as lubricating ball-bearings between these larger particles. A gradation which is in low VMA or excessive asphalt binder content also shows the same effect. For ensuring acceptable aggregate gradation, gradation specifications are used. Table 3.2 shows the aggregate gradation of the mix design.

Table 3.2
Summary of Aggregate Characteristics from Mix Design

Gradation (% passing)	Blend	Virgin
5/8”	100	100
1/2”	96.4	96.3
3/8”	86.2	85.3
#4	63.2	61.5
#8	44.4	42.7
#16	33.2	32.0
#30	21.5	20.4
#50	12.8	12.0
#100	7.3	6.6
#200	5.4	5.0

Table 3.3

Properties of the Mix Design

Virgin Add AC (%)	4.1
Virgin Agg. FAA (%)	42.9
Asphalt Absorption (%)	1.12
Water Absorption (%)	1.85
Light Wt Particles (%)	2.3
Toughness (% Loss)	NA

3.3 Compaction

The following procedures were followed for compacting fiber and no-fiber specimens:

- The loose mixes were reheated at 290°F
- Heated loose mixes were compacted in the lab using gyratory compactor to prepare samples at 7± 1% air voids for testing.
- Both fiber and no fiber samples are compacted using gyratory compactor at 75 mm and 100 mm height.

3.3.1 Gyratory Compactor

In the Gyratory Compaction technique, a cylindrical mold of a bituminous mixture is taken and is subjected to two simultaneous forces : a vertical static compacting force and a shear force induced by rotating the mold on its inclined axis. Compaction data is then recorded from the measured values.

Operating Principle

The gyratory compaction technique is used to:

- prepare specimens of a given density and height, for testing mechanical properties in subsequent steps
- derive the ration of curve density to gyration amount
- determine for a given amount of gyrations, the void content of the sample.

During gyratory compaction, the two forces of shearing action and static compression produce a movement in the center line of the sample. This produces a surface of revolution that is conical in shape. The ends of the sample stay perpendicular to the conical surface axis.

By compacting conventional mixes, 25 samples were made in the laboratory. Table 3.4 shows the compaction data for the conventional mixes.

Table 3.4
Compaction data for conventional mixes

Sample No.	**Mass Weight (g)**	**Specimen Height (mm)**	**Vertical Pressure (KPa)**	**No. Revolutions**	**Uncorrected Gmm (%)**
1	2924.00	74.99	604.17	29	90.8
2	2942.00	74.94	603.18	43	90.9
3	2932.00	74.89	602.93	33	91.2
4	2830.00	74.73	602.19	12	91.1
5	2930.50	74.84	601.20	28	69.3
6	2930.2	74.84	600.95	30	91.2
7	2931.8	74.94	600.2	26	91.2
8	2931	74.89	601.2	27	91.1
9	2932.5	74.75	600.7	29	91.2
10	2932	74.84	599.21	33	91.2
11	2926.3	74.84	597.23	44	91
12	2930	74.84	596.98	32	91.1
13	2933.4	74.84	599.21	24	91.2
14	2927.2	74.78	604.17	21	91.1
15	2930.5	74.84	600.7	26	91.1
16	2930	74.84	601.2	26	91.1
17	2927.6	74.68	602.93	23	91.2
18	2928	74.89	602.2	26	91.1
19	2931	74.78	603.68	27	91.1
20	2928.1	74.78	597.97	28	91.1
21	3923.3	99.57	604.92	21	91.7
22	3918.8	99.59	602.68	21	91.5
23	3920	99.54	599.71	24	89.6
24	3922.3	99.7	597.97	23	89.5
25	2915	74.78	600.2	11	89.2

By compacting fiber-reinforced mixes, 23 samples were made in the laboratory. Table 3.5 shows the compaction data for the fiber - reinforced mixes.

Table 3.5
Compaction Data for Fiber-Reinforced Mixes

Sample No.	Mass Weight (g)	Specimen Height (mm)	Vertical Pressure (Kpa)	No. Revolutions	Uncorrected Gmm (%)
1F	2937.20	74.72	601.20	27	91.20
2F	2920.40	74.73	599.21	21	91.20
3F	2944.30	74.73	600.45	26	91.20
4F	2943.80	74.68	601.20	21	91.30
5F	2940.1	74.84	599.71	31	91.2
6F	2940.5	74.78	598.47	26	91.1
7F	2940.2	74.84	600.2	28	91.2
8F	2940.6	74.73	598.47	24	91.2
9F	2940.3	74.84	604.6	40	91.4
10F	2935	74.89	604.42	26	91.3
11F	2542	74.53	604.67	2	79.3
12F	2540	74.84	600.7	23	79
13F	2948	74.84	600.45	33	91.7
14F	2541.8	74.73	598.22	26	91.7
15F	2546.5	74.78	599.21	27	79.2
16F	2949.2	74.78	598.47	28	91.8
17F	2942	74.94	601.2	30	91.5
18F	2943	74.84	600.95	38	91.5
19F	2943	74.89	599.46	38	91.5
20F	3914.5	100	604.67	21	90.2
21F	3920	100	600.2	20	90.2
22F	3914.5	100	604.67	21	90.2
23F	3920	100	600.2	20	90.2

3.4 Volumetric Properties

3.4.1 Bulk Specific Gravity(G_{mb})

Specific gravity is the ratio of the density of a material to the density of water at $73.4°F$.. At $73.4°F$, water's specific gravity is thus 1.

In the laboratory, the bulk specific gravity is the specific gravity of the sample with respect to the same volume of water.

While testing a HMA specimen for determining Bulk specific gravity, three conditions are considered as follows:

- Measuring dry weight of the sample (no water should be in the sample).
- Measuring saturated surface dry weight of the sample (SSD, water fills the HMA air voids)
- Measuring weight of the submerged sample in water (underwater).

The bulk specific gravity can then be calculated using the three quantities measured above.

Water Displacement Methods have been used for determining Bulk Specific gravity of the prepared non-fiber and fiber samples. The volume of the sample has been calculated by doing subtraction of the mass of the sample in water from that of the SSD sample. In the SSD state, the air voids internal to the sample are completely filled with water while the surface of the sample is completely dry. In the SSD state, air voids internal to the sample considered to be a part of the sample volume. The SSD state is attained by first immersing the sample in water for about four minutes.

The sample is then removed from the water and the surface dried with a towel that is damp.

In the laboratory, the samples were first dried to a constant mass and cooled to room temperature. The dry masses were then recorded as shown in figure 3.1.

Figure 3.1. Recording the dry mass

For 4 minutes, the sample was submerged in 77°F water and the mass recorded. A water filled container was used to measure this.

This setup is shown in figure 3.2. The sample was then blotted with a towel and the dry mass was recorded.

The Bulk Specific Gravity G_{mb} was calculated using

$$G_{mb} = \frac{A}{(B - C)} \tag{3.1}$$

Figure 3.2. Submerging sample for 4 minutes and recording submerged mass

where B is mass of SSD sample in air, A is the mass of sample in air, and C is mass of sample in water. The water absorption was calculated by

$$waterabsorption = \left(\frac{B-A}{B-C}\right) \times 100 \tag{3.2}$$

3.4.2 Maximum Specific Gravity (G_{mm})

Maximum Specific Gravity (G_{mm}) is defined as the specific gravity of a HMA where air voids are excluded. In other words, the combined specific gravity of the asphalt binder and the remaining aggregate after the air voids are all removed from the HMA sample is the maximum specific gravity. This value when multiplied by water

density ($1000g/L$ or $62.4lb/ft^3$) gives the Theoretical Maximum Density which is also known as Rice density(Rice, 1957).

Maximum specific gravity is a crucial property of HMA as it is required in the calculation of air void percentage in the compacted HMA sample. This is required in both the design of Superpave mixes and also the to find the air void percentage in field tests. G_{mm} is calculated by

$$G_{mm} = \frac{A}{(A + D - E)} \tag{3.3}$$

where A is the mass of the sample in air, D is the flask mass when filled with water, and E is the combined flask mass and sample when filled with water.

3.4.3 Air Voids (V_a)

Aid voids (V_a) is defined as the percentage by volume of all the air pockets trapped between the aggregate particles in the compacted mixture to the total volume of the mixture. Air voids are an important measurement as it is one of the determining factors of pavement durability and stability. In a typical dense grade mix which has about 12.5 mm maximum aggregate size, air voids eight percent and above give rise to a water-permeable mixture while three percent and below give rise to unstable mixtures.

The volume of air voids in the pavement mixture is given by

$$V_a = \left(1 - \frac{G_{mb}}{G_{mm}}\right) \times 100 \tag{3.4}$$

whereG_{mm} is the maximum specific gravity of the sample and G_{mb} is the bulk specific gravity of the sample.

Calculation of Bulk specific gravity G_{mb} and air voids for 25 Conventional specimens and 23 fiber specimens has been shown in Table 3.6 and Table 3.7. G_{mm} value for mix design 2.434 was provided by NDDOT. G_{mm} value 2.482 was determined in the laboratory conducting Rice test on the loose mixes.

Table 3.6
Air Voids Determination for Conventional Mixes (Gmm is based on ND-DOT mix design or UND Rice)

Sample No	Dry Weight (g)	Wet Weight (g)	SSD Weight (g)	G_{mb}	G_{mm} (Mix, Rice)	Air Voids (%) (Mix, Rice)	Test
1	2911.40	1651.70	2938.90	2.262	2.434, 2.482	7.07, 8.86	SCB
2	2938.20	1662.70	2459.00	2.267	2.434, 2.482	6.86, 8.66	DCT, SCB
3	2919.90	1659.90	2945.60	2.271	2.434, 2.482	6.70, 8.50	
4	2817.50	1567.70	2861.00	2.178	2.434, 2.482	10.52, 12.25	
5	2925.5	1673	2960.5	2.272	2.434, 2.482	6.65, 8.46	
6	2920.5	1667.4	2951.8	2.274	2.434, 2.482	6.57, 8.38	DCT, SCB
7	2918.6	1658.1	2958.1	2.245	2.434, 2.482	7.76, 9.55	
8	2911.4	1654.7	2946.8	2.253	2.434, 2.482	7.44, 9.23	
9	2890.4	1653.8	2926.8	2.27	2.434, 2.482	6.74, 8.54	
10	2924.5	1669.5	2961.1	2.264	2.434, 2.482	6.98, 8.78	APA
11	2911	1667.4	2946.9	2.275	2.434, 2.482	6.53, 8.34	APA
12	2888.1	1636.9	2927.6	2.238	2.434, 2.482	8.05, 9.83	
13	2907	1643.8	2942.1	2.239	2.434, 2.482	8.01, 9.79	
14	2885	1638	2926	2.239	2.434, 2.482	8.00, 9.79	
15	2907.3	1651.2	2944.6	2.248	2.434, 2.482	7.64, 9.43	DCT
16	2949	1678	2975.4	2.273	2.434, 2.482	6.61, 8.42	DCT
17	2913.8	1647.1	2937.9	2.257	2.434, 2.482	7.27 9.07	DCT
18	2904.4	1670.2	2947.8	2.273	2.434, 2.482	6.61, 8.42	DCT
19	2933.3	1661.6	2957.3	2.264	2.434, 2.482	6.98, 8.78	APA
20	2946.6	1672.5	2972.2	2.267	2.434, 2.482	6.86, 8.66	APA
21	190.9	1081.9	1931	2.241	2.434, 2.482	7.93, 9.71	DCT
22	3884.7	2199.6	3930	2.245	2.434, 2.482	7.76, 9.55	DCT
23	3899.9	2220	3947.5	2.257	2.434, 2.482	7.27, 9.07	DCT
24	3912.5	2229.8	3959.8	2.261	2.434, 2.482	7.11, 8.90	DCT
25	2828.8	1582	2880.7	2.178	2.434, 2.482	10.52, 12.25	Not Used

Table 3.7
Air Voids Determination for Fiber-Reinforced Mixes (Gmm is based on NDDOT mix design or UND Rice)

Sample No	Dry Weight (g)	Wet Weight (g)	SSD weight (g)	Gmb	Gmm (Mix, Rice)	Air Voids (%) (Mix, Rice)	Test
1F	2948.6	1654.4	2963.9	2.251	2.434, 2.465	7.52, 8.68	
2F	2914.3	1630.4	2939.9	2.225	2.434, 2.465	8.59, 9.74	
3F	2943.5	1649.8	2955.9	2.254	2.434, 2.465	7.39, 8.56	APA
4F	2923.2	1646.8	2948.9	2.245	2.434, 2.465	7.76, 8.92	
5F	2947	1669.8	2967.1	2.272	2.434, 2.465	6.65, 7.83	APA
6F	2944	1668.6	2969.1	2.264	2.434, 2.465	6.98, 8.15	APA
7F	2935.1	1659.2	2958.5	2.259	2.434, 2.465	7.19, 8.36	APA
8F	2934.2	1657.6	2958.4	2.256	2.434, 2.465	7.31, 8.48	DCT, SCB
9F	2986.1	1701.1	2997.3	2.304	2.434, 2.465	5.34, 6.53	
10F	2912.8	1646.2	2939.4	2.252	2.434, 2.465	7.47, 8.64	DCT, SCB
11F	2557.6	1437	2679.8	2.058	2.434, 2.465	15.4, 16.51	
12F	2939.6	1662.8	2965.6	2.256	2.434, 2.465	7.31, 8.48	DCT, SCB
13F	2940.2	1674.6	2963.6	2.281	2.434, 2.465	6.28, 7.46	
14F	2933.7	1666.3	2961.3	2.265	2.434, 2.465	6.94, 8.11	
15F	2946.9	1672.8	2973.4	2.266	2.434, 2.465	6.9, 8.07	
16F	2937	1667.8	2963.5	2.267	2.434, 2.465	6.86, 8.03	DCT, SCB
17F	2929.4	1662	2959.7	2.257	2.434, 2.465	7.27, 8.44	
18F	2932.2	1660.4	2960	2.256	2.434, 2.465	7.31, 8.48	
19F	2945.1	1673.1	2974.6	2.262	2.434, 2.465	7.07, 8.24	DCT
20F	3923	2208.1	3944.6	2.259	2.434, 2.465	7.19, 8.36	DCT
21F	3921	2203.6	3946.9	2.249	2.434, 2.465	7.608.76	DCT
22F	3923	2208.1	3944.6	2.259	2.434, 2.465	7.19, 8.36	DCT
23F	3921	2203.6	3946.9	2.249	2.434, 2.465	7.60, 8.76	DCT

3.5 Testing

3.5.1 Asphalt Pavement Analyzer (APA)

The Asphalt Pavement Analyzer is used for mix design test which provides an empirical testing of the asphalt mixes during the design stage. The APA is one of the several loaded wheel testers which provides accelerated performance testing of asphalt mixes. Rutting of asphalt pavement is a significant issue for municipal pavement infrastructure. The APA is an important tester used to assess the rutting resistance of HMA materials. APA is widely used in United States and Canada in the evaluation of rutting potential of the mixes. The APA machine has also additional features for evaluating fatigue cracking and moisture susceptibility of the mixes in different conditions(Kandhal and Cooley, 2003).

The APA is a loaded wheel tester. For the application of repetitive load through a rubber hose, the APA has pneumatic cylinders attached to a concave metal wheel. 8000 strokes or repetitions are usually applied on the HMA specimens. The generated contact pressure can be up to 1378 kPa but for stimulating actual field loading conditions, a contact pressure of 690 kPa is typically used. The APA system has built in deformation , contact pressure measurement and also calibration of load.

The APA test machine can work with three sets of two cylindrical samples or three beam samples. Beam samples usually have dimensions 300 mm x 100 mm x 75 mm. Cylindrical samples are made with a diameter of 150mm and thickness of 75 mm. To use cylindrical samples smaller than 75m, shimming is used. The tests are conducted in a test chamber that has a controlled environment. The test

temperatures are typically selected to mimic the environmental conditions in the field. To select the temperature for the test, the temperature of the location of the project is used(Kandhal and Cooley, 2003).

The APA tester outputs the average measured deformation of two cylindrical samples or three positions on each of the beam samples. Figure 3.3 depicts a graphical output from a typical test of the APA(Kandhal and Cooley, 2003). Figure 3.3 graph shows that after 8000 cycles or strokes the final average deformation of the specimen which is identified as rut depth is 4.94 mm.

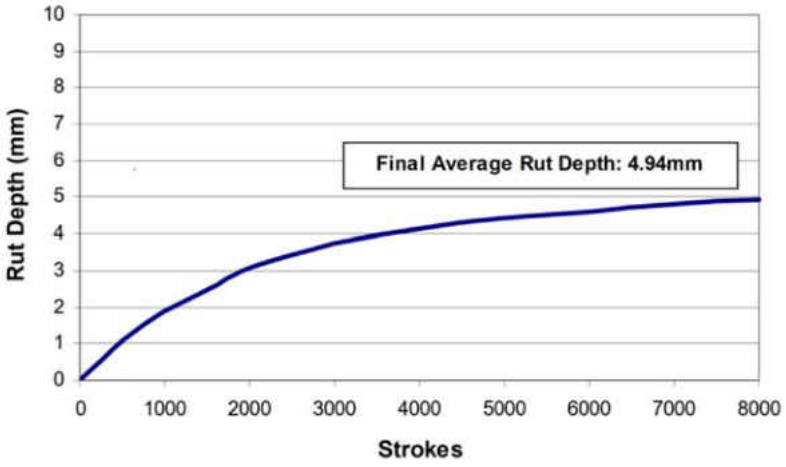

Figure 3.3. Typical APA output(Kandhal and Cooley, 2003)

3.5.2 Disc Shaped Compact Tension(DCT) Test

The fracture energy of a typical asphalt sample is obtained using the Disk-Shaped Compact Test(DCT) tester. This test setup is able to test cylindrical cores extracted

from asphalt pavement samples in-place or samples that have undergone gyratory compaction created in the process of mix design(Wagoner et al., 2005).

Figure 3.4 shows that The specimen has a circular geometry with loading holes on each side of the notch. This geometry can maximize the fracture area and is thereby able to reduce the geometry-associated variability of test results. However, as mentioned by Wagoner et al. (2005), this test is able to record the transformation of asphalt mixes from being a brittle material at cold temperatures and becoming increasingly ductile with greater temperatures.

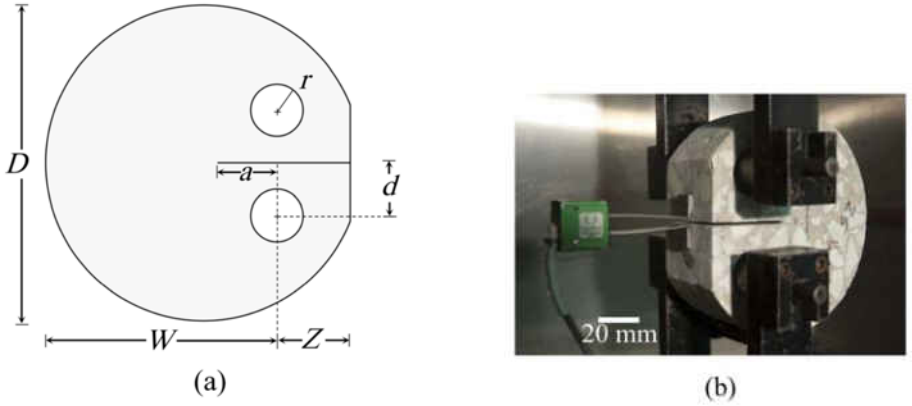

(a) (b)

Figure 3.4. (a) DCT Geometry[] (b) DCT Setup Configuration[]

A typical test of asphalt using the DCT test involves the testing of the surface at different load rates and temperatures. The range of fluctuations in the fracture energy is acquired from the DCT test and is compared with the range of values acquired from other tests. When the test is able to detect fracture energy changes under different conditions of testing, the DCT geometry can potentially be used (Park et al., 2015).

3.5.3 Semi Circular Bend (SCB) Test

In the Semi Circular Bend test, a semi-circular sample with a notch is subjected to a three-point bending test. This results in tension in the bottom of the specimen which in turn propagates cracks throughout the sample. Owing to the fact that the sample preparation is simple, the SCB test is used to evaluate fracture properties of samples compacted in the laboratory and also for samples extracted from the field. Compared to DCT, the SCB test has smaller potential fracture surface. However, since the geometry is semi-circular, twice as many samples can be tested at a given time. Mixed mode fracture behavior of asphalt can be easily characterized just by the adjustment of the angle of inclination of the notch (Im et al., 2014).

3.5.4 Preparation of samples for APA test

- For APA tests 75 mm samples were used and after 8 hours of testing rutting results for both fiber and no fiber specimen are obtained.
- APA samples were conditioned in the APA at 58°F for 5 hours before testing.
- Tables 3.6 and 3.7 show the samples that were ultimately chosen for the APA results.

3.5.5 Preparation of samples for DCT and SCB test

DCT and SCB samples were cut and/or drilled according to specifications. For DCT and SCB tests 75 mm samples were cut into 2 pieces as 50 mm and 25 mm

samples where 50 mm sample are used for DCT and 25 mm sample for SCB. The crack for DCT was cut to about 50-55mm depth. DCT samples were conditioned for six hours at -18°C before testing. The crack for SCB samples was cut to about 15-20 mm depth. Samples for SCB test were conditioned for two hours at 19°C before testing.

Figure 3.5. Pictures of DCT samples being loaded into DCT machine

CHAPTER 4

RESULTS AND DISCUSSION

Three sets of test results have been discussed in this section.

1. APA's rut resistance results as deformations under the wheel loads (hoses) of the APA (in millimeters)

2. DCT's low-temperature cracking results as fracture energy (Joules/m2) at maximum loading (in kN); and

3. SCB's fracture energy results (Joules/m2) at max loading (in kN) and the flexibility indices.

Results are discussed int the following sections:

4.1 Rutting Resistance Results

The APA was loaded with four samples. For each run, two samples were put on the left side hose and the other two at the middle hose. The conventional mix samples and the fiber-reinforced samples were alternated between the left and middle hoses to minimize the effect of testing under a different hose. At the end, we ran enough samples to choose samples tested under the same hose (the middle hose was chosen in this case) to completely eliminated hose induced variability. Table 4.1 and Figure 4.1 display the APA rut resistance results. Please note that the APA measures

Table 4.1
Rut Results for Conventional and Fiber-Reinforced Samples

Mix Type	Conv.	Conv.	Conv.	Conv.	Fiber	Fiber	Fiber	Fiber
Sample No	10	10	11	11	6F	6F	5F	5F
@ 8000 Cycles	1.2933	1.2372	1.2634	1.2484	2.1193	2.1343	2.1268	2.1044
@ 30 Cycles	-0.1047	-0.3289	-1.4203	-1.3344	0.4261	0.4186	0.3962	0.1383
Rut Values	1.3979	1.5661	2.6837	2.5828	1.6932	1.7156	1.7306	1.9661
Ave Rut Value per Sample (mm)	1.48		2.63		1.70		1.85	
Mix Type	Conv.	Conv.	Conv.	Conv.	Fiber	Fiber	Fiber	Fiber
Sample No	19	19	20	20	3F	3F	7F	7F
@ 8000 Cycles	1.5771	1.6369	1.8088	1.4613	1.8053	1.7754	1.7754	1.7530
@ 30 Cycles	0.1869	0.0374	0.2691	-0.0112	0.4037	0.2729	0.0411	-0.2915
Rut Values	1.3902	1.5995	1.5397	1.4725	1.4017	1.5026	1.7343	2.0446
Ave Rut Value per Sample (mm)	1.49		1.51		1.45		1.89	

deformation under the hose at two locations under each sample (@ 1/3 the distance from each end of the sample). The rut (deformation values) are recorded for each of the 8000 cycles of loading. The first 30 cycles were ignored for seating the sample. The difference between the rut value at 8000 cycles and 30 cycles is reported as the rut value under the hose. The average of the two rut values for each sample are then reported as the rut value for one sample.

The rutting values shown in Table 4.1 were mostly below 2 mm across the board, which is considered very low. Normally, rut values up to 5 mm are considered excellent. This indicates that mix design from project NHU-SS-TRP-2-020(016)001 near

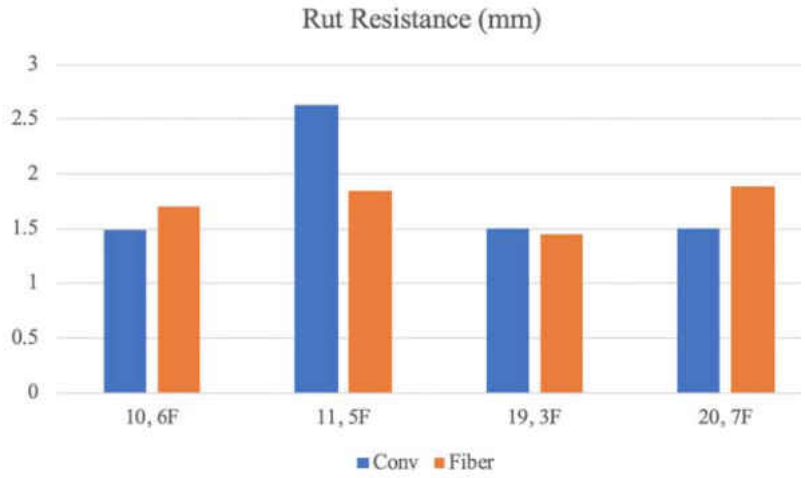

Figure 4.1. Average Rut Results for Conventional and Fiber-Reinforced Samples

Valley City was excellent. The average rut value for all four specimens for the conventional and fiber-reinforced mixes were 1.779mm and 1.723mm, respectively. The fiber-reinforced average is lower than the conventional mix average by 3%. It would be safe to say that fiber increases rut resistance by 3%, or at least it would not decrease rut resistance of the conventional mix.

Figure 4.2 displays the rut deformations of samples from conventional and fiber-reinforced mixes.

Figure 4.2. Display of APA Samples after Rutting Conventional Mixes (left) and for Fiber-Reinforced Mixes (right)

4.2 DCT Low Temperature Cracking Results

The summary results for the DCT are shown in Table 4.2. Table 4.2 includes the following information: sample no., fracture energy in J/m^2, maximum load (kN), and air void values (%) for the tested specimens. Please note that the letter "F" next to a number indicates that the sample belongs to a fiber-reinforced mix. The shaded areas indicate the additional testing results to confirm results. Also figure 4.3 shows the before and after test shape of the sample.

Figure 4.3. DCT Sample: (a) Ready for Testing (left), (b) Test Completed (right)

A quick look at Table 4.2 shows that 10 DCT samples were initially tested. Initially 5 non-fiber samples (17,15,2,18,6) and 5 fiber samples (8F,19F,10F,12F,16F) were tested for DCT test. Since the results came out counter to expectations, additional 8 samples were constructed and tested (4 samples for fiber-reinforced mixes were-20F,21F,22F,23F mixes and 4 samples for conventional mixes were - 21,22,23,24). These additional 8 samples were tested later to confirm the earlier results. The overall average of the conventional mix energy is 553.6 J/m^2, while the average for the overall average for the fiber-reinforced mix was 440.4 J/m^2, which means the energy for fiber-reinforced mix is about 20% lower than the conventional mix.

Table 4.2
Fracture Energy and Maximum load Results for Conventional and Fiber-Reinforced Samples

Sample No.	Energy (J/m^2)	Max Load (kN)	Air Voids (%) NDDOT Mix	Air Voids (%) UND Rice
17	333	4.043	7.27	9.07
15	392	3.857	7.64	9.43
2	699	0.739	6.86	8.66
18	730	0.72	7.31	8.42
6	912	0.769	6.57	8.38
21	374	3.237	7.93	9.71
22	580	2.996	7.76	9.55
23	494	2.78	7.27	9.07
24	468	2.1	7.11	8.9
8F	314	3.06	7.31	8.48
19F	421	3.904	7.07	8.24
10F	448	3.56	7.47	8.64
16F	556	4.238	6.61	8.03
12F	729	0.643	7.31	8.48
20F	352	3.492	7.19	8.36
21F	331	3.077	7.60	8.76
22F	378	2.670	7.19	8.36
23F	435	2.873	7.60	8.76

Fracture energy that has been obtained during DCT test for Non-fiber and Fiber samples are shown in the figures 4.4 and 4.5 respectively.

Figure 4.4 shows the fracture energy graph for non-fiber sample no.2 where the test temperature was -18C and the fracture energy for this sample was 699 J/m2 where maximum load was0.739 kN at 61.92 seconds.

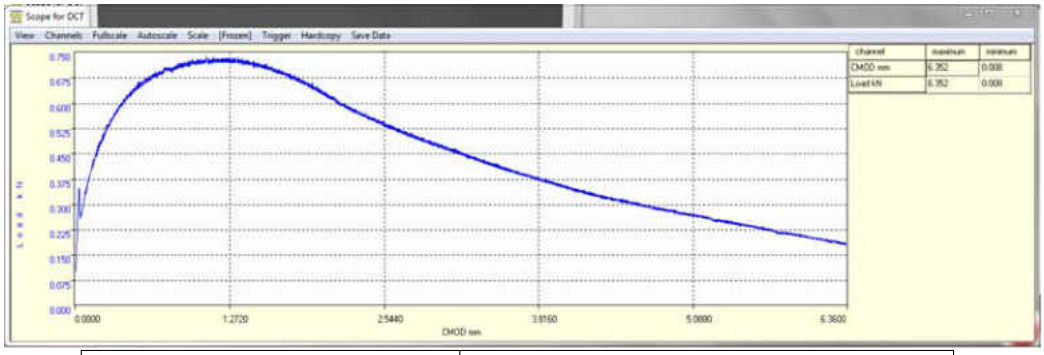

Specimen ID	Non-fiber 2
Test temperature	-18C
Diameter	150.00 mm
Thickness	47.00 mm
Energy	699 J/m^2
Cumulative Area	2857.72 N-mm
Slope	0.0170 mm/second
Max Load	0.739 kN at 61.92 seconds
Ave Temperature	-17.9 C
Test Duration	371.92 seconds

Figure 4.4. Fracture energy graph for non-fiber sample no. 2.

Figure 4.5 shows the fracture energy graph for fiber sample no. 10F where the test temperature was -18C and the fracture energy for this sample was 448 J/m2 at where maximum load was3.560kN at 9.60 seconds.

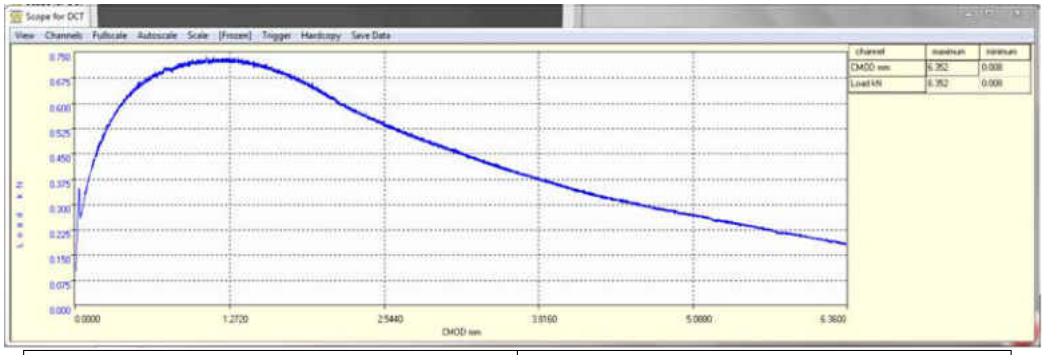

Specimen ID	fiber 10F
Test temperature	-18C
Diameter	150.00 mm
Thickness	47.00 mm
Energy	448 J/m^2
Cumulative Area	1831.17 N-mm
Slope	0.0170 mm/second
Max Load	3.560 kN at 9.60seconds
Ave Temperature	-17.4 C
Test Duration	131.84 seconds

Figure 4.5. Fracture energy graph for fiber sample no. 10F

The current guidelines by the University of Illinois indicate that fracture energy of at least 400 J/m^2 are sufficient for low traffic level volumes ($<$ 10 Million ESALs); fracture energy of at least 460 J/m^2 for medium traffic level volumes (10-30 Million ESALs); and fracture energy of at least 690 J/m^2 for high traffic volumes ($>$ 30 Million ESALs)[].

By comparing the fracture energy results of this study to the University of Illinois guidelines, both the fiber-reinforced and the conventional mixes are approximately sufficient for up to 30 million ESALs. Remember that all samples were tested at -18°C, which is a 10°C higher than the low-end temperature of the PG 58-28 used as stated in the testing protocol.

4.3 SCB Fatigue Cracking Results and Discussions

The raw data of the SCB test has been processed by the FIT software which was developed by the University of Illinois Urbana-Champagne. A summary of the SCB. Fatigue cracking results that were obtained during tests are given in Table 4.3.

Table 4.3
Fracture Energy, Maximum load, and Flexibility Index Results for Conventional and Fiber-Reinforced Samples

Sample No.	Energy (J/m^2)	Max Load (kN)	Flexibility Index	Air Voids (%)
1(2)	931.76	0.874	12.59	7.07
6(1)	824.45	0.771	2.9	6.57
6(2)	879.81	0.770	10.6	6.57
8F(1)	1284.63	1.004	11.89	7.31
8F(2)	1723.52	1.162	10.08	7.31
10F(1)	1677.88	0.887	10.97	7.47
16F(2)	1723.52	1.162	10.08	6.86

Figure 4.6 shows the fracture energy graph for non-fiber sample no. 1 where the fracture energy for the sample is 931.76 J/m2 where the inflection point found at displacement 1.422700e+00 mm and load 5.182038e-01 kN.

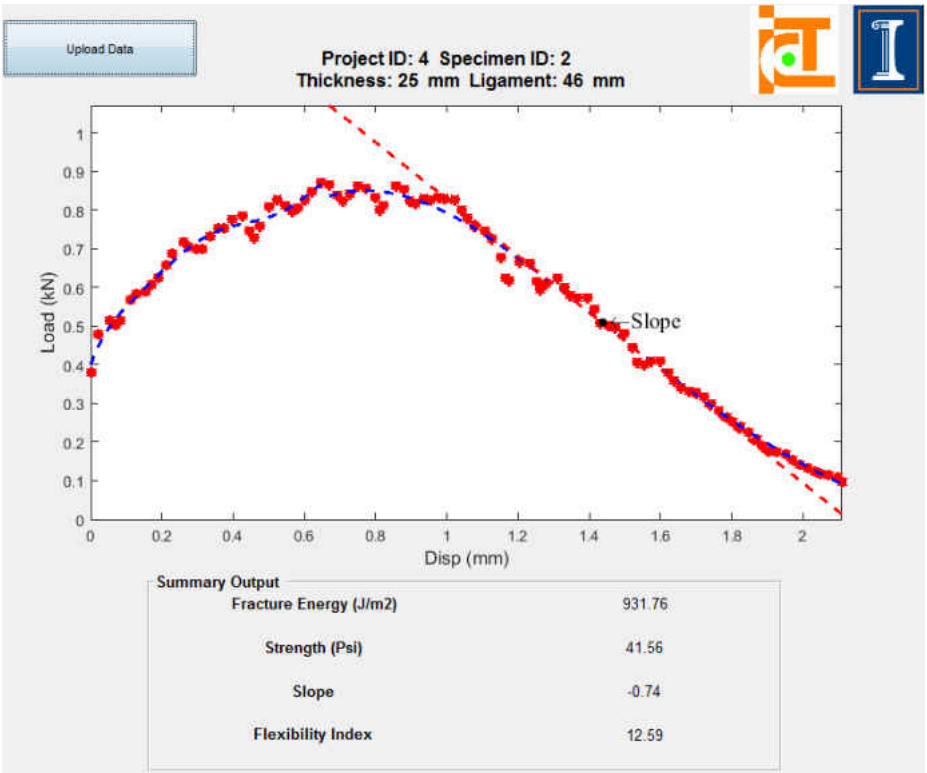

Figure 4.6. Fracture energy of non-fiber Sample no. 1

Figure 4.7 shows the fracture energy graph for non-fiber sample no. 6 where the fracture energy for the sample is 879.81 J/m2 where the inflection point found at displacement 2.564100e+00 mm and load 4.430496e-01 kN.

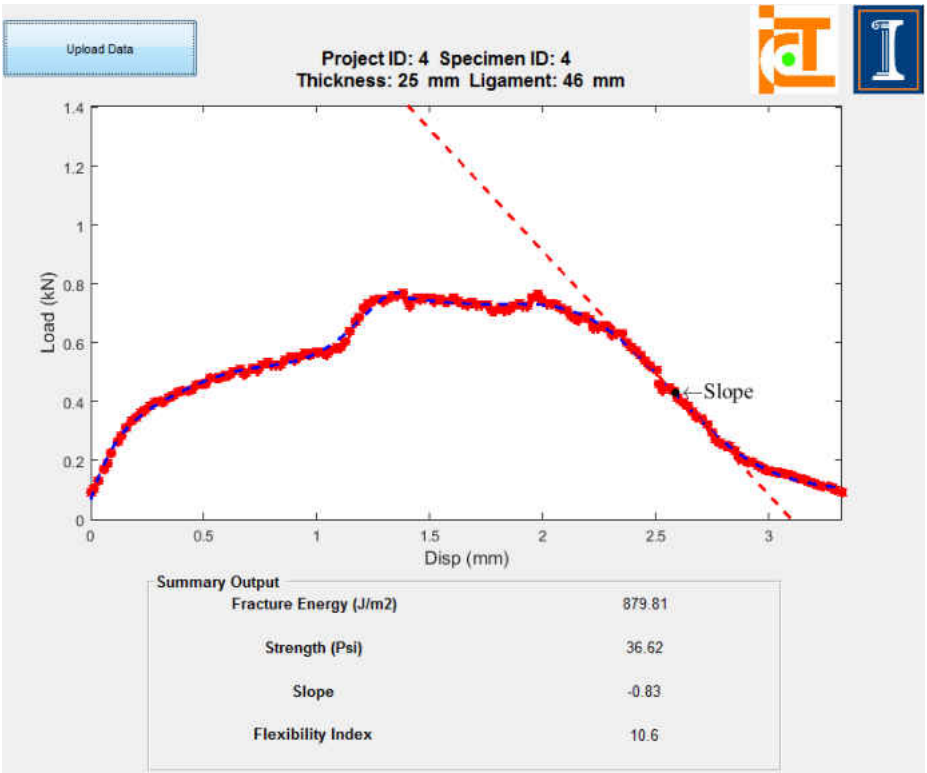

Figure 4.7. Fracture energy of non-fiber Sample no. 6

Figure 4.8 shows the fracture energy graph for fiber sample no. 10F where the fracture energy for the sample is 1677.88 J/m2 where the inflection point found at displacement 3.087700e+00 mm and load 2.730557e-01 kN.

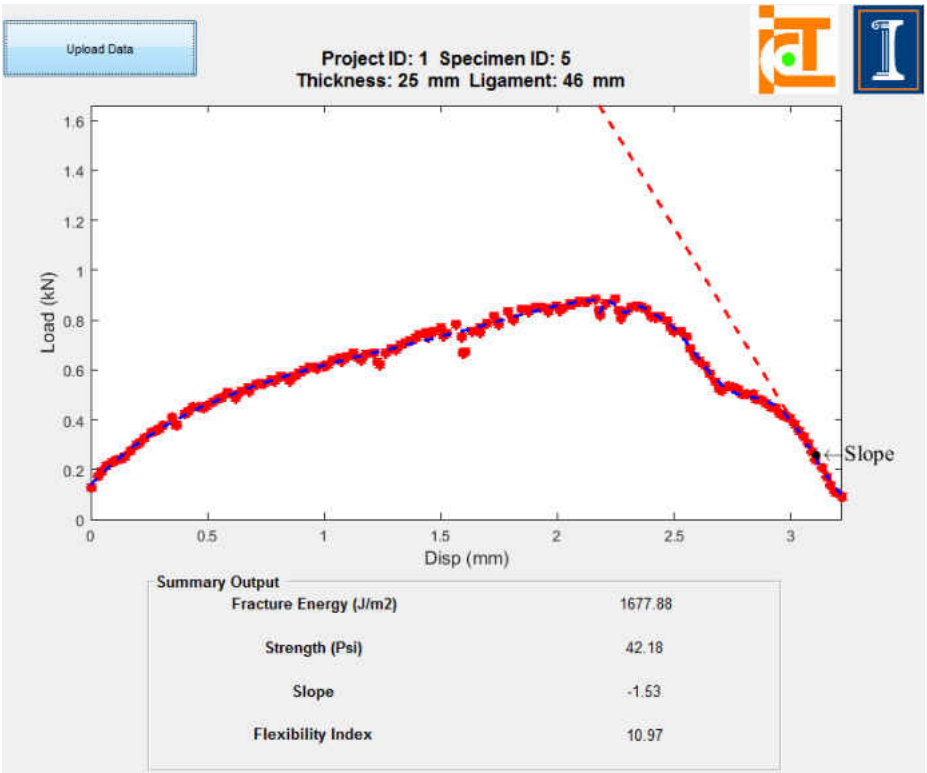

Figure 4.8. Fracture energy of non-fiber Sample no. 10F

Figure 4.9 shows the fracture energy graph for fiber sample no. 16F where the fracture energy for the sample is 1723.52 J/m2 where the inflection point found at displacement 2.529500e+00 mm and load 6.703368e-01 kN.

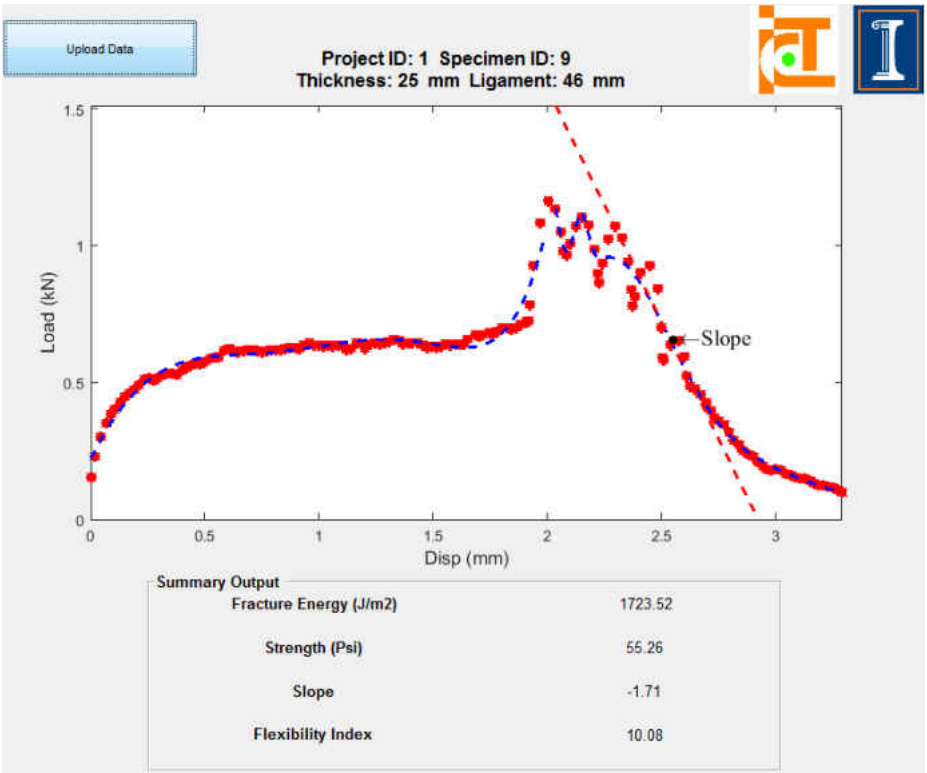

Figure 4.9. Fracture energy of non-fiber Sample no. 16F(2)

For the SCB test, the average cracking energy for the conventional and fiber-reinforced mixes were 879 and 1602 , respectively. Both mixes have high fracture energy but obviously, the addition of fiber has improved the fracture energy by 82.4%. Before cracking sample and sample after cracking test has been illustrated in figure 4.10

Figure 4.10. SCB Sample: (a) Ready for Testing (left), (b) Test Completed (right)

CHAPTER 5

CONCLUSIONS AND RECOMMENDATIONS

The addition of Aramid fiber to a SuperPave HMA has improved the rutting resistance by at least three percent. For low temperature cracking, the DCT test showed that the addition of fiber decreased the fracture energy responsible for low temperature cracking by about 20%, which is a detriment not an improvement. On the other hand, the addition of Aramid fiber did increase the fracture energy responsible for fatigue cracking (related to traffic loading) by 82%.

5.1 Limitations and Future Work

5.1.1 Limitations

While compacting loose mixes to prepare non-fiber and fiber specimen, the temperature might not be exactly at 290°F due to practical errors. The percentage of Aramid fiber on the fiber mixes was not mentioned by the NDDOT. While preparing and cutting the conventional sample no. 6 for SCB test, the 15 mm cut for the sample might not be precise for which the test result shows anomaly in the flexibility index. Asphalt content percentage in the loose mixes might be affected due to reheating.

5.1.2 Future Recommendation

Further investigation should be done to investigate why the addition of aramid fiber decreased the fracture energy responsible for low temperature cracking. Rejuvenators can be added along with fiber to the mix to investigate if the low temperature cracking resistance can be improved.

Bibliography

AlphaPavingTexas (2019 (accessed July 1, 2019)). *What is Asphalt Fatigue Cracking.* `https://www.alphapavingtexas.com/faq/asphalt-fatigue-cracking/`.

Brown, J. H. and Maurer, B. A. (1989). Macroecology: the division of food and space among species on continents. *Science*, 243(4895):1145–1150.

Fu, S.-Y., Lauke, B., Mäder, E., Yue, C.-Y., and Hu, X. (2000). Tensile properties of short-glass-fiber-and short-carbon-fiber-reinforced polypropylene composites. *Composites Part A: Applied Science and Manufacturing*, 31(10):1117–1125.

Huet, C. (1990). Application of variational concepts to size effects in elastic heterogeneous bodies. *Journal of the Mechanics and Physics of Solids*, 38(6):813–841.

Im, S., Ban, H., and Kim, Y.-R. (2014). Characterization of mode-i and mode-ii fracture properties of fine aggregate matrix using a semicircular specimen geometry. *Construction and Building Materials*, 52:413–421.

Kandhal, P. S. and Cooley, L. A. (2003). *Accelerated laboratory rutting tests: Evaluation of the asphalt pavement analyzer*, volume 508. Transportation Research Board.

Kandhal, P. S., Foo, K. Y., and Mallick, R. B. (1998). Critical review of voids in mineral aggregate requirements in superpave. *Transportation Research Record*, 1609(1):21–27.

Liley, C. (February 2018). Rutting: Causes, prevention, and repairs. *Illinois Asphalt Pavement Association*.

Mahrez, A., Karim, M., and Katman, H. (2003). Prospect of using glass fiber reinforced bituminous mixes. *Journal of the Eastern Asia Society for Transportation Studies*, 5:794–807.

Marasteanu, M., Zofka, A., Turos, M., Li, X., Velasquez, R., Li, X., Buttlar, W., Paulino, G., Braham, A., Dave, E., et al. (2007). Investigation of low temperature cracking in asphalt pavements national pooled fund study 776.

Muftah, A., Bahadori, A., Bayomy, F., and Kassem, E. (2017). Fiber-reinforced hot-mix asphalt: Idaho case study. *Transportation Research Record*, 2633(1):98–107.

Park, P., El-Tawil, S., Park, S.-Y., and Naaman, A. E. (2015). Cracking resistance of fiber reinforced asphalt concrete at- 20 c. *Construction and Building Materials*, 81:47–57.

PavementInteractive (2019 (accessed July 1, 2019)b). *Pavement Distresses*. `https://www.pavementinteractive.org/reference-desk/pavement-management/pavement-distresses/`.

PavementInteractive (2019 (accessed July 10, 2019)a). *Fatigue Cracking*. https://www.pavementinteractive.org/reference-desk/pavement-management/pavement-distresses/fatigue-cracking/.

Rice, J. (1957). Maximum specific gravity of bituminous mixtures by vacuum saturation procedure. In *Symposium on Specific Gravity of Bituminous Coated Aggregates*. ASTM International.

Roberts, F. L., Kandhal, P. S., Brown, E. R., Lee, D.-Y., and Kennedy, T. W. (1991). Hot mix asphalt materials, mixture design and construction.

Serfass, J. and Samanos, J. (1996). Fiber-modified asphalt concrete characteristics, applications and behavior. *Asphalt Paving Technology*, 65:193–230.

Tech, S. (2019 (accessed July 1, 2019)). *Surface Tech*. https://surface-tech.com/.

Wagoner, M. P., Buttlar, W. G., and Paulino, G. H. (2005). Development of a single-edge notched beam test for asphalt concrete mixtures. *Journal of Testing and Evaluation*, 33(6):452–460.

Wikipedia (2019 (accessed July 1, 2019)). *Rut_roads*. https://en.wikipedia.org/wiki/Rut_roads.

Xu, Q., Chen, H., and Prozzi, J. A. (2010). Performance of fiber reinforced asphalt concrete under environmental temperature and water effects. *Construction and Building materials*, 24(10):2003–2010.

Zumrawi, M. M. and Edrees, S. A. S. (2016). Comparison of marshall and superpave asphalt design methods for sudan pavement mixes.

APPENDIX

HOT MIX DESIGN DATA - SUPERPAVE

Department of Transportation, Materials and Research (Rev. 3-16) 9/25/17

Mix Design Company: Knife River Materials

Lab. No.	
Location	Jamestown North
Project	NHU-SS-TRP-2-020(016)001
	PCN 18853
District	Valley City
County	Stutsman
Date	9/25/17
Pit Owner(s)	Councilman, Paul
Pit #1 Location	34-143-66 & 3-142-66
Pit #2 Location	
Pit #3 Location	

Project Specification	Section 430
Type of AC (top lift)	58-28
Type of AC (bot lift)	58-28
Letting Date	12/15/16
Plus #4 (%)	36.8
Minus #4 (%)	63.2

Gyratory Compactive Effort

Ninitial	7
Ndesign	75
Nmaximum	115

Mix Properties at Recommended Asphalt Content

	Mix Design	Specification
Optimum AC (%)	5.5	NA
Density (pcf)	145.8	NA
Air Voids (%)	4.0	2.0-6.0
VMA (%)	14.1	14.0min
VFA (%)	71.3	65-78
%Gmm @ Ninitial	88.3	89max
%Gmm @ Nmaximum	97.1	98max
AC Film Thickness (m)	8.1	7.5-13.0
Dust/Effective AC Ratio	1.2	.6-1.3
Fine Agg Angularity (%)	43.0	43min
Sand Equivalent (%)	54.3	40min
Coarse Agg Angularity (%)	89.3	75min
Flat/Elongated Pieces (%)	0.0	10max

Maximum SpG @ Ndes 2.434

Summary of Aggregate Characteristics from Mix Design

Gradation (% passing)	Blend	Virgin
5/8"	100.0	100.0
1/2"	96.4	96.3
3/8"	86.2	85.3
#4	63.2	61.5
#8	44.4	42.7
#16	33.2	32.0
#30	21.5	20.4
#50	12.8	12.0
#100	7.3	6.6
#200	5.4	5.0

Virgin Add AC (%)	4.1
Virgin Agg. FAA (%)	42.9
Asphalt Absorption (%)	1.12
Water Absorption (%)	1.85
Light Wt Particles (%)	2.3
Toughness (% Loss)	NA

Final Aggregate Blend (%)

22	N Fines	Councilman
20	Rock	Councilman
28	ASD	Councilman
10	W fines	Councilman
20	RAP	

Specific Gravity Information

Combined Bulk (Gsb)	2.570
-No. 4 Combined Bulk (Gsb)	2.548
-No. 4 Virgin Bulk (Gsb)	2.530
Apparent (Gsa)	2.720
Effective (Gme)	2.643

Remarks:

Mix Design Technician & ID: Danny Schmidt #1366

Distribution:
Materials and Research
Valley City

Figure 1. PG58-28 HMA Mix Design Summary